Statistical Modeling of 60 GHz Wireless Channel in an Underground Mine Gallery

Shah Ahsanuzzaman Md Tariq*, Charles Despins†, Sofiène Affes‡ and Chahé Nerguizian*

*École Polytechnique de Montréal, Montreal, Canada
†PROMPT-Quebec, Montreal, Canada
‡INRS-EMT, Université du Québec, Montreal, Canada
Emails: tariq.shah-ahsanuzzaman-md@polymtl.ca, CDespins@promptinc.org,
affes@emt.inrs.ca, chahe.nerguizian@polymtl.ca

***Abstract*—In this work, 60 GHz radio wave propagation measurements at 40 m underground mine gallery and its statistical modeling are presented. Different antennas such as horn and omnidirectional with horizontal (H) and vertical (V) polarizations employing 0.46 ns time resolution have been considered during the campaign. Results that vertical polarization, a higher number of multipath higher RMS (root mean square) delay spread value horizontal polarization. Statistical modeling of multipath profiles that path arrival follows the modified Poisson distribution while path amplitude satisfies mostly the Lognormal distribution.**

***Index Terms*—60 GHz wideband channel measurement, underground mine, polarization, path amplitude, path arrival.**

I. Introduction

60 GHz frequency band is recently studied for high data rate short range wireless local area network (WLAN) application [1]–[3]. Its 7 GHz unlicensed bandwidth between 57 and 64 GHz has special characteristics such as high oxygen absorption loss and less interference. This frequency band is driving underground wireless communication applications such as geolocation, video, voice communication, automation as well as security. Measurements and statistical modeling of this kind of environment are required for system designers in order to simulate the channel and predict the performance.

More than a decade, LRTCS-UQAT laboratory, located in Val-d'Or, has measurement campaigns to improve mining industry wireless communication system [4]–[6]. The experimental mine CANMET for campaign, is different from offices and corridors, since it consists of rough surfaces which can be affected by reflections and scattering at the particular wavelength of 5 mm. Therefore, channel characteristic and modeling are necessary for wireless system design in underground mine. Nerguizian et al. [4] found 27 ns RMS delay spread at 2.4 GHz and Boutin et al. [6] compared measurement results between 2.4 GHz and 5.8 GHz reporting no correlation of RMS delay spread and no clustering effect of impulse responses with respect to distances. Moreover, results of path arrival and path amplitude followed modified Poisson distribution and Rice distribution, respectively for LOS condition. At 60 GHz, path loss and capacity analysis have been investigated in [7].

Deterministic modeling such as ray tracing typically used to model millimetre wave channel in indoor environments [2], [8]. In underground mine is not realistic due to scattering phenomena, however, a feasible solution could be statistical modeling based on experimental results. Statistical parameters of path amplitudes and path arrivals obtained from multipath profiles are sufficient to generate simulated impulse responses in this particular environment [6]. In this paper, 60 GHz frequency with different antenna configuration amplitudes and arrivals with different antenna polarizations are investigated.

In section II, we will address the measurement setup and the experimental protocol. Section III expose the results based on some relevant parameters extracted from the measurement data related to statistical modeling. Finally, conclusion is presented in the last section.

II. Measurement setup and experimental protocol

In CANMET experimental mine, a measurements zone at 40 m level gallery is used. The dimension of the mine level is approximately 5 m in both height and width. The floor is mostly flat which consists large slopes in the tangent plane and full of dry dust covered with small rock particles. The ceilings are especially rougher and covered with metallic net. Gallery walls are mostly rough and consist of sharp edges. From the wall roughness measurements, the estimate roughness (standard deviation) 6 cm and the maximum and the average roughness thickness are around 37 cm and 20 cm, respectively [9]. The humidity and the temperature were 100 percent and 6 degrees, respectively. The 40 m underground mine level is shown in Fig.1.

Fig. 1. 40 m mine gallery

978-1-4673-6555-0/15/$31.00 ©2015 IEEE

In order to find channel impulse responses, a 60 GHz frequency domain wideband measurement system setup has been used. A Vector Network Analyzer (ANRITSU MS 4647A) with a frequency band ranging from 40 MHz to 70 GHz has been employed. Gain of 30 dB for the Power Amplifier (CBM 57653/015-03 CERNEX) and a 4 m cable with 7.86 dB/m loss at the transmitter, in conjunction with Low Noise Amplifier (CBL 57653/055-01 CERNEX) and another 4 m cable at the receiver have been considered in the setup. A second Low Noise Amplifier (QuinStar, Serial N11328, Model 001001) has been added, with a gain of 18 dB, to enhance the signal at the receiver. The bandwidth of the signal was 2.16 GHz between a frequency range of 57.24 GHz to 59.4 GHz. Transmitter power was set to +4 dBm. The system calibration was with 2000 frequency sweep points with a sample frequency of 1.08 GHz. Directional and vertically polarized pyramidal horn antennas with 24 dBi gain and half-power beam width (HPBW) of around 12° in azimuth and in elevation planes were used. A vertically polarized Omnidirectional antenna with 3 dBi gain and HPBW of 360° in azimuth and -10° to 40° in elevation directions has been used. The heights of the transmitter and the receiver were approximately 1.5 m. An ideal measurements' setup was conducted with Omni-Horn ($O-H$) configuration with horizontal (H) and vertical (V) polarizations. The polarization of the antenna has been changed from V to H manually using a shift of 90°. A camera tripod and a laser were used during measurements of the quasi-static (no movements of people) wireless channel in order to have the accurate position of LOS condition. The data acquisition was completed by connecting a computer to the VNA via a GPIB interface. A Velmex table having the capability to do a small fraction of $\lambda/2$ steps of the receiver along the x direction has been used. A Labview program was employed to control the whole measurement procedure.

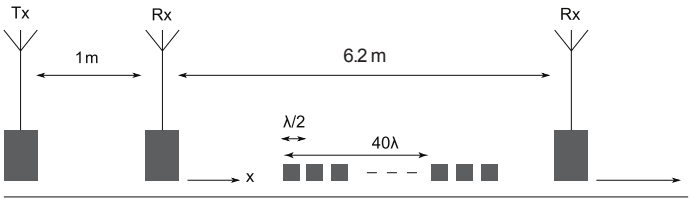

Fig. 2. Mmeasurement procedure where an omnidirectional antenna and a directional horn antenna were used as Tx and Rx, respectively.

The data collected during measurements have been used for statistical modeling described in section III. Transmitter and receiver were aligned the receiver was moved every 40λ along the LOS condition (i.e. x direction) form 1 m to 7.2 m distance as shown in Fig. 2. At each position, three consecutive measurements were taken separated by $\lambda/2$ with 15 snapshots different observation time instances. Far field of the horn and omnidirectional antenna set as 1 m. To remove the antenna effect and the system losses from the channel, data from 1 m measurements have been used.

Using the inverse Fourier transform (IFFT), the time domain normalized magnitude with 0.46 ns time resolution of the complex impulse responses was obtained from the recorded frequency responses using the procedure employed in [6]. Therefore, for a position d, the measured channel impulse response $h(\tau; d)$ different time instances have been obtained PDPs $P(\tau; d) = |h(\tau; d)|^2$. Noise threshold was then selected after careful inspection of maximum delay of multipath all profiles. Its value was set by a dynamic threshold as described in [10].

III. Statistical modeling

Statistical characteristics of wireless channel propagation in underground mine and tunnels are site specific and depend on the employed frequency band. Recent surveys of wireless communications and propagation modeling in underground mines and tunnels have been reported in [11]–[13]. Several approaches to model typical environment such as numerical methods for Maxwell equation, wave guide and ray approach are noticed in [14]–[17]. A theoretical and a ray optical theory have been developed by Ndoh et al. [18] and Fono et al. [19], respectively. Prediction of amplitude, arrival time and the RMS delay spread were modelled both in narrow band and wide band cases using the theoretical ray optical method in [15]. As in open literature, waveguide approach gives analytical solution for smooth walls and ceiling. Since the surface roughness of the underground mine is higher than the wavelength, and the gallery walls contain metallic pipes, nets, arches preventing collapse and various kinds of objects mounted on the walls and ceiling, ray tracing approach might not be appropriate since large number of reflected, diffracted and scattered rays and higher computational time. As reference, radio wave propagation modeling approaches using electromagnetic theory for rectangular, circular, semicircular tunnels might be useful. However, the problem can be partially solved for the best fitted approach so far by using a hybrid modeling approach or empirical based statistical model for multipath simulation. Statistical model can be obtained by using empirical multipath arrivals and amplitudes [6].

A. Path arrival modeling

A simple path arrival model is a Poisson process which can characterize the random arrivals of paths [8]. Some studies in indoor and underground mine environments suggest that modified Poisson distribution fit with empirical measurement results as described in [20] and [6]. This phenomena can be explained that the arrival of paths are not totally random (e.g., fixed average arrival rate λ), it can be Poisson process where probability of having a path in index i is given by λ_i (e.g., individual arrival rate of paths) [8]. Fig. 3 illustrates the probability of path occupancy for 40 $\mathrm{m}_{H-O_{VV}}$ and 40 $\mathrm{m}_{H-O_{HH}}$ configuration for each path index of 0.46 ns delay. Results show that in the first path index the probability of having a path is 1 for both configurations. It can be noticed that for the second path index no path arrivals observed in both configurations, since the path index delay time resolution (i.e., 1/BW) is lower than the second path arrival time coming

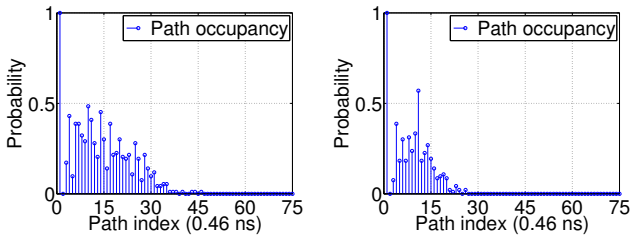

(a) (b)

Fig. 3. Probability of path occupancy as a function of path index with different antenna polarization configurations. (a) and (b) are the 40 $m_{O-H_{VV}}$ and 40 $m_{O-H_{HH}}$ configurations, respectively.

from the surfaces of the galleries. The results from the 3rd to maximum number of path index, provide the probability of having a path is decreases gradually until the maximum path delay. Moreover, result shows that the probability of having path in VV configuration is higher than HH. Fig. 4 shows the distribution of the number of paths occurrence for 2^{nd} to 5^{th}, 10^{th}, 15^{th} and 20^{th} path index, respectively, where path arrival of first index is always present. The comparison between empirical results with poission, modified poission and weibull distribution and corresponding minimum mean square error (MMSE) values are shown in Fig. 5. The results suggest that the modified poission distribution offers the best fit for both antenna polarization configurations.

B. Path amplitude modeling

The amplitude fluctuations of each path can be classified into Rayleigh, Rice, Nakagami, Weibul and Lognormal distributions. The linear relative amplitudes of each path index are determined and compared with the theoretical five distributions by using Kolmogorov-Smirnov (KS) test. The KS test results identify the best fitted distribution and results show that each path index follow Lognormal distribution, since higher bandwidth (i.e., 2.16 GHz) causes average of received signal power over a wide frequency spectrum which makes stable signal strength [8]. An example of the amplitude distributions of first path index of different polarization configurations is shown in Fig. 6. Zhang [21] reported that if an LOS propagation path exists, along with a limited number of multipath components the lognormal distribution can be applied [22]. The mean and standard deviation of the amplitudes of each bin are then fitted with a curve fitting technique expressed as $y = y_0 + ae^{xb}$. Where y_0 and a are the constants, b is the decay rate and x is the vector of path indexes. The fitting results are listed in table I. The exponential curve fitting of mean and standard deviation of the normalized path amplitudes as a function of path index is shown in Fig. 7.

Results show that the received power is concentrated in the initial path and presents slow and faster rate of decays. Slower decay rate has been observed in VV polarization both in mean and standard deviation of path amplitudes compared to HH polarization. This can be explained by the fact that the vertically polarized omnidirectional antenna covers 360°

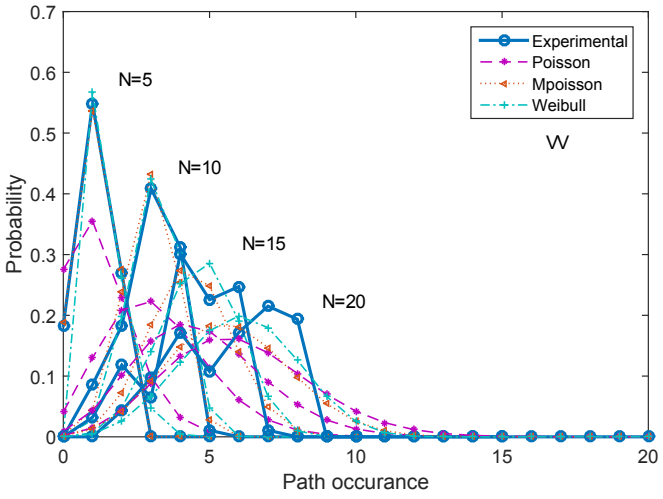

(a)

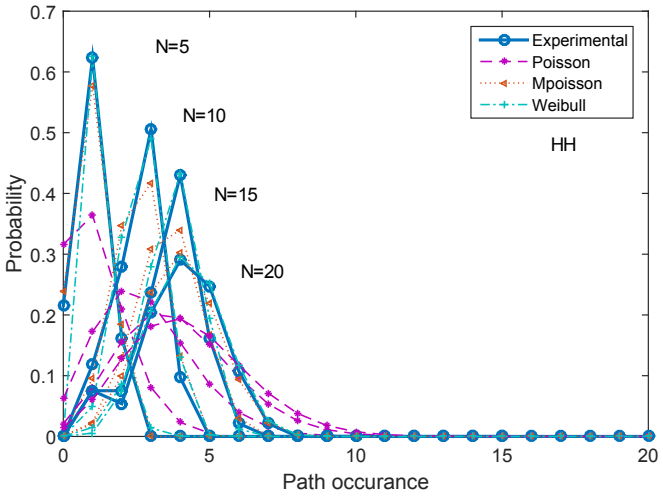

(b)

Fig. 4. Path arrival distribution, where N in the total number of considered path indexes without considering the first path occurrence at first path index. (a) and (b) are the VV and HH configurations, respectively.

TABLE I
PATH AMPLITUDE MODEL PARAMETERS

Configuration	Mean			Standard deviation		
	y_0	a	b	y_0	a	b
40 $m_{O-H_{VV}}$	-1.34993E-7	0.51262	-0.1515	-0.00373	0.10059	-0.05076
40 $m_{O-H_{HH}}$	-3.1573E-9	0.27231	-0.18273	-0.00118	0.07592	-0.0813

indicating higher number of multipath components with higher amplitude and delay. It can be noticed that close to the 10^{th} path index, the mean and standard deviation of path amplitudes are higher than the neighbouring path indexes.

C. Simulation of impulse responses

Three steps are followed to simulate the impulse responses of the underground mine channel from the statistical modeling of path arrivals and amplitudes. Firstly, the path arrival of all indexes are generated followed by the best fitted distribution which is modified Poisson with its optimal parameters of the

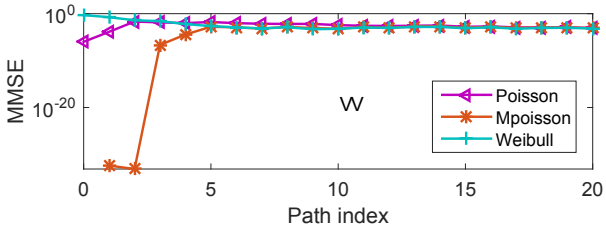

(a)

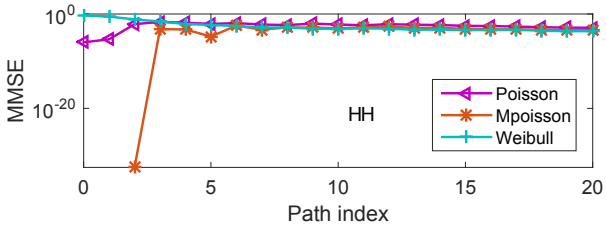

(b)

Fig. 5. The MMSE of three distributions compare to measurement results. (a) and (b) are the VV and HH configurations, respectively.

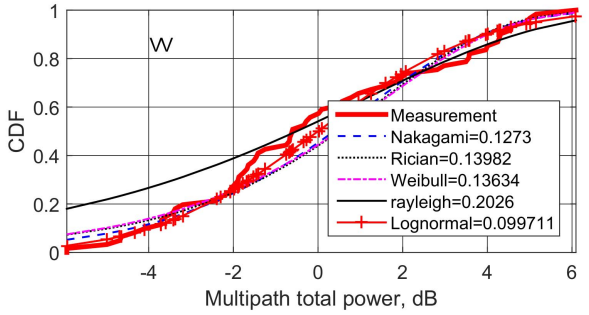

(a)

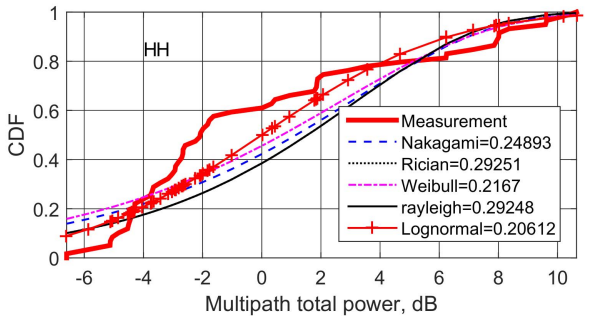

(b)

Fig. 6. An Kolmogorov-Smirnov (KS) test and corresponding K values of the path amplitudes at the first path index. (a) and (b) are the VV and HH configurations, respectively.

constant K as described in [20] and [6]. Secondly, the five sets of amplitude distribution following Rayleigh, Rice, Nakagami, Weibul and Lognormal with the statistical parameters of each path index are generated. Finally, each generated path arrival model is combined with five sets of amplitude distributions. The RMS delay spread (τ_{rms}) values have been extracted from the power delay profiles as described in [10]. The mean

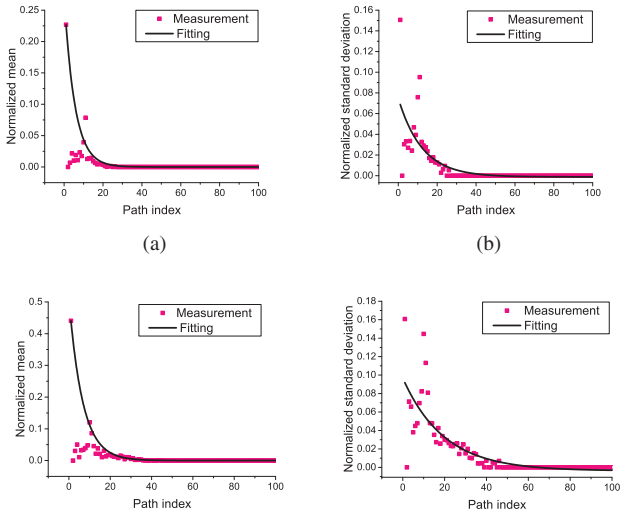

(a) (b) (c) (d)

Fig. 7. The normalized mean and standard deviation of the amplitudes with different polarization configurations. (a) and (b) are the mean and standard deviation of 40 $m_{O-H_{HH}}$, (c) and (d) are the mean and standard deviation of 40 $m_{O-H_{VV}}$, respectively.

values of the τ_{rms} are found to be 2.63 ns and 2.04 ns for 40 $m_{O-H_{VV}}$ and 40 $m_{O-H_{HH}}$, respectively. Then the empirical RMS distribution is compared with each simulated RMS distribution of five amplitude models by using KS test. The KS test results show that the Lognormal distribution for the amplitude is the best fitted amplitude distribution. An example of this test and corresponding k values for 40 $m_{O-H_{VV}}$ configuration is shown in Fig. 8. The 500 simu-

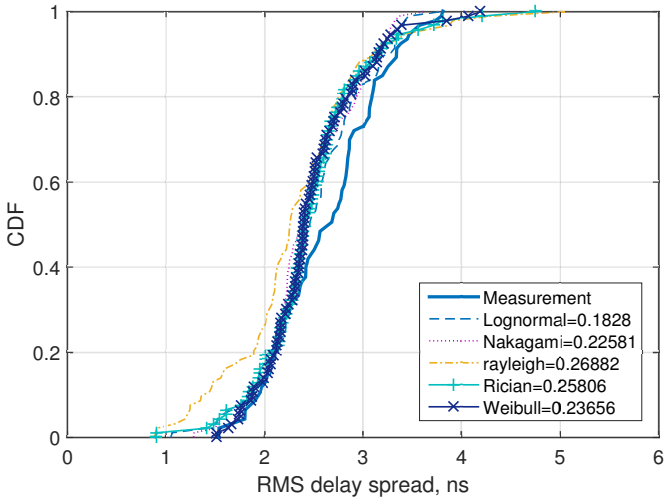

Fig. 8. An example of Kolmogorov-Smirnov (KS) test and corresponding K values between measured and simulated RMS delay spread of 40 $m_{O-H_{VV}}$ configuration.

lated RMS delay spread with these five amplitude models are then compared with the experimental RMS delay spread, using the Kolmogorov-Smirnov test to identify the best performance

of the models. The performance with the fitted statistical parameters is given in Table II. The performance scores show that the Lognormal is the best fit of amplitude model and modified Poisson distribution is the best fit for path arrival model.

TABLE II
PERFORMANCE RESULTS COMPARED TO EXPERIMENTAL τ_{rms}

40 m	Omni-Horn (HH)	Omni-Horn (VV)
Lognormal	226	205
Nakagami	44	110
Rayleigh	83	53
Rician	115	59
Weibull	32	73

IV. CONCLUSIONS

This paper presents a measurement campaign and the statistical wireless channel modeling at 60 GHz for an underground mine at 40 m level depths. Time dispersion parameter were extracted, and path amplitude and path arrival of different antenna polarizations are investigated.

Statistical simulation of impulse responses were conducted and compared with measured impulse responses based on RMS delay spread. Performance results suggest that the Lognormal distribution matches better for multipath amplitude distribution and modified poission distribution performs best fits for the multipath arrivals. Results also show a little or no clustering of path amplitudes observed in both configurations.

These measurement results can be used subsequently to build an empirical model based on statistical parameters for underground mine wireless channel in the 60 GHz band.

REFERENCES

[1] T. Rappaport, R. Heath, R. Daniels, and J. Murdock, *Millimeter Wave Wireless Communications*, ser. Prentice Hall Communications Engineering and Emerging Technologies Series. Prentice Hall, 2014.

[2] S. K. Yong, P. Xia, and A. V. Garcia, *60 GHz Technology for Gbps WLAN and WPAN: From Theory to Practice*. Wiley, 2011.

[3] P. F. Smulders, "Statistical characterization of 60 GHz indoor radio channels," *IEEE Transactions on Antennas and Propagation*, vol. 57, no. 10 PART 1, pp. 2820 – 2829, 2009.

[4] C. Nerguizian, C. L. Despins, S. Affes, and M. Djadel, "Radio-channel characterization of an underground mine at 2.4 GHz," *IEEE Transactions on Wireless Communications*, vol. 4, no. 5, pp. 2441–2453, 2005.

[5] Y. Rissafi, L. Talbi, and M. Ghaddar, "Experimental characterization of an UWB propagation channel in underground mines," *IEEE Transactions on Antennas and Propagation*, vol. 60, no. 1, pp. 240 – 246, 2012.

[6] M. Boutin, A. Benzakour, C. L. Despins, and S. Affes, "Radio wave characterization and modeling in underground mine tunnels," *IEEE Transactions on Antennas and Propagation*, vol. 56, no. 2, pp. 540 – 549, 2008.

[7] M. El Khaled, P. Fortier, and M. Ammari, "A performance study of line-of-sight millimeter-wave underground mine channel," *IEEE Antennas and Wireless Propagation Letters*, vol. 13, pp. 1148–1151, 2014.

[8] K. Pahlavan and A. Levesque, *Wireless Information Networks*, ser. Wiley Series in Telecommunications and Signal Processing. Wiley, 2005.

[9] S. Ahsanuzzaman Md Tariq, C. Despins, S. Affes, and C. Nerguizian, "Rough surface scattering analysis at 60 GHz in an underground mine gallery," in *2014 IEEE International Conference on Communications Workshops (ICC)*, June 2014, pp. 724–729.

[10] A. Benzakour, S. Affes, C. Despins, and P.-M. Tardif, "Wideband measurements of channel characteristics at 2.4 and 5.8 GHz in underground mining environments," in *Vehicular Technology Conference, 2004. VTC2004-Fall. 2004 IEEE 60th*, vol. 5, Sept 2004, pp. 3595–3599.

[11] A. Forooshani, S. Bashir, D. Michelson, and S. Noghanian, "A survey of wireless communications and propagation modeling in underground mines," *IEEE Communications Surveys Tutorials*, vol. 15, no. 4, pp. 1524–1545, Fourth 2013.

[12] S. Yarkan, S. Guuzelgooz, H. Arslan, and R. Murphy, "Underground mine communications: A survey," *IEEE Communications Surveys Tutorials*, vol. 11, no. 3, pp. 125–142, rd 2009.

[13] A. Hrovat, G. Kandus, and T. Javornik, "A survey of radio propagation modeling for tunnels," *IEEE Communications Surveys Tutorials*, vol. 16, no. 2, pp. 658–669, Second 2014.

[14] M. Ndoh and G. Delisle, "Underground mines wireless propagation modeling," in *IEEE 60th Vehicular Technology Conference, 2004. VTC2004-Fall. 2004*, vol. 5, Sept 2004, pp. 3584–3588 Vol. 5.

[15] Y.-P. Zhang, Y. Hwang, and R. Kouyoumjian, "Ray-optical prediction of radio-wave propagation characteristics in tunnel environments. 2. analysis and measurements," *IEEE Transactions on Antennas and Propagation*, vol. 46, no. 9, pp. 1337–1345, Sep 1998.

[16] Z. Sun and I. Akyildiz, "Channel modeling and analysis for wireless networks in underground mines and road tunnels," *IEEE Transactions on Communications*, vol. 58, no. 6, pp. 1758–1768, June 2010.

[17] G. Ke, Z. Zhangdui, B. Ai, R. He, B. Chen, Y. Li, and C. Briso Rodriguez, "Complete propagation model in tunnels," *IEEE Antennas and Wireless Propagation Letters*, vol. 12, pp. 741–744, 2013.

[18] M. Ndoh, G. Delisle, and R. Le, "An approach to propagation prediction in a complex mine environment," in *17th International Conference on Applied Electromagnetics and Communications, ICECom 2003*, Oct 2003, pp. 237–240.

[19] V. Fono, L. Talbi, and N. Hakem, "Propagation modeling in complex rough environment based on ray tracing," in *2013 IEEE Antennas and Propagation Society International Symposium (APSURSI)*, July 2013, pp. 1924–1925.

[20] R. Ganesh and K. Pahlavan, "Statistical modelling and computer simulation of indoor radio channel," *IEE Proceedings I Communications, Speech and Vision*, vol. 138, no. 3, pp. 153–161, June 1991.

[21] W. Zhang and N. Moayeri, "Classification of statistical channel models for local multipoint distribution service using antenna height and directivity," in *IEEE 802.16.1pc-00/07*, 2000.

[22] J. Schothier, "WP3-study: the 60 GHz channel and its modelling," in *IST-2001-32686 Broadway*.